J Therm Anal Calorim (2010) 102:729–737
DOI 10.1007/s10973-010-0864-z

Microcalorimetric determination of effect of the antioxidant (Quercetin) on polymer/surfactant interactions

Kulbir Singh · D. Gerrard Marangoni

Received: 25 May 2009 / Accepted: 4 May 2010 / Published online: 11 June 2010

Abstract Isothermal titration calorimetry (ITC) and batch calorimetry techniques have been used to evaluate the effect of added antioxidant (Quercetin, QN) on the binding between a polymer/surfactant complex, namely the sodium salt of polystyrene sulfonate (PSS) and typical anionic surfactant sodium dodecylsulfate (SDS). An indirect isotherm approximation method and the Satake–Yang model have been used to evaluate the binding parameter (Ku), adsorption cooperativity (u), and the Gibbs free energy of cooperative and non-cooperative binding (ΔG_C and ΔG_N) from the ITC data. The enthalpy of dissolution of QN into various PSS/water and PSS/SDS/water solutions has been evaluated from batch calorimetry to study the energetics of the polymer/surfactant binding in the presence of QN.

Keywords Isothermal titration calorimetry (ITC) · Batch calorimetry · Polymer/surfactant · Antioxidant · Quercetin

Introduction

Interactions between ionic polymers and surfactants have been intensely studied in both the polymer and the surfactant literature, due to interest in both academic and industrial research programs [1]. Polymer/surfactant complexes and the interactions that lead to complex formation are relevant in biological systems and processes and have applications in cosmetics, pharmaceuticals, and a host of other industrial fields. Isothermal titration calorimetry (ITC) has been successfully applied unraveling the subtle balance of intermolecular forces that lead to the formation of polymer/surfactant complexes. ITC measures the enthalpy (heat flow) per injection as the titrant (e.g., surfactant molecules) is titrated into a polymer solution. In recent years, ITC has been used in the characterization of surfactant/polyelectrolyte interactions where it has been used to determine critical aggregation concentrations (cac) [2, 3], study the association mechanism [4], and to evaluate the thermodynamic parameters (e.g., Gibbs free energy, enthalpy, and entropy) of many binding processes. ITC has also been used to measure binding isotherms for other systems such as ligand binding to protein polymers [5–7], and colloidal particles [8]. A significant advantage in using ITC to measure binding isotherms is that the thermodynamic functions of binding (namely, ΔH, ΔS, and ΔG) can be determined directly. Hence, in a single experiment, the energetics behind polymer/surfactant interactions can be readily determined.

Flavonoids are polyphenolic compounds that occur in many species in the plant kingdom [9, 10]. Flavonoids have attracted attention recently due to the fact that these compounds have been shown to possess excellent therapeutic characteristics, including acute high potency and low systemic toxicity. Quercetin (3,5,7,3′,4′-pentahydroxyflavone; see Fig. 1) is one of the most common flavonoids present in nature. Quercetin is well known for its potent antioxidant behavior and metal ion chelating capacity; hence, it possesses a variety of biological and biochemical effects including anti-inflammatory, antineoplastic, and cardioprotective activities [11–15]. However, in order to gain a full understanding of the modes of action of bioflavonoids like quercetin, the study of their interactions with a number

K. Singh · D. G. Marangoni (✉)
Department of Chemistry, St Francis Xavier University, P.O. Box 5000, Antigonish, NS B2G 2W5, Canada
e-mail: gmarango@stfx.ca; g_marangoni@colloid.stfx.ca

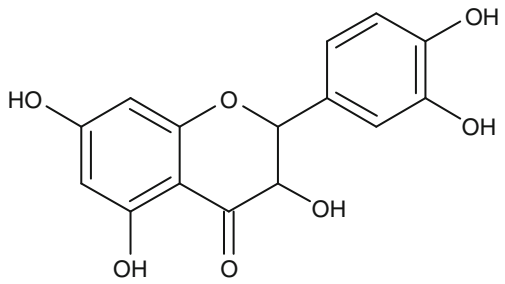

Fig. 1 Structure of the quercetin molecule

of biologically relevant model systems, including nucleic acids [16], enzymes [17], and other proteins [18], is required.

The polyphenolic structure of quercetin makes it very sensitive to changes in its environment, which may alter its solubility, hydrophobicity, and electrochemical properties, and may also affect its antioxidant capacity. Thus, investigation of the interaction of quercetin with molecularly self-assembled systems (e.g., micelles) formed by different surfactants is of fundamental importance. Micelles are often used as model systems for cell membranes. Hence, understanding the interaction of these bioflavonoid molecules with different surfactants can yield valuable information on the manner in which quercetin can interact with various cell membranes [14–18].

Studies related to the interaction of polyphenolic compounds, such as tannin, with biopolymers like proteins have also been undertaken [19] and are of importance in the food sciences and the pharmaceutical industry [20]. The low water solubility of quercetin necessitates a sensitive technique for probing the interactions between the bioflavonoid and the model membrane systems. Additionally, given the fact that Hayakawa et al. have found that a hydrophobic, water insoluble dye enhanced the binding of surfactant ions to the polymer, [1] it is of interest to examine the effect of sparingly soluble quercetin in water on polymer/surfactant binding by using calorimetric techniques. There are a number of papers in the literature where calorimetry has been used to examine polymer/surfactant systems [21–24], thermodynamic of micelle formation [25–27], surfactant adsorption [4, 28–32], polymer micelles [33], and binding in biomaterials [7, 34–37]. In this article, the effect of added quercetin on the binding of an anionic surfactant to a polyelectrolyte is investigated by isothermal titration calorimetry. The raw calorimetric data are fitted to the two-binding-state Satake–Yang adsorption model, which quantifies the extent of binding in terms of binding constant (Ku) and cooperativity parameter (u). The results are expected to provide an understanding of the effect of quercetin solubilization on the ligand/polyelectrolyte interactions.

Experimental

Materials

Sodium dodecylsulfate (SDS), sodium polystyrenesulfonate (PSS, mol.wt. 500000), and quercetin (QN, flavonoid) having purities of 99, 95, and 99%, respectively were purchased from Sigma Aldrich. All chemicals were used as received. All solutions were prepared by mass using triply deionized water, obtained from a Millipore ion-exchange system.

Sample preparation

Standard saturated QN solutions were made by dissolving an excess of QN (2 mg) in PSS solutions with varying PSS concentrations (0.5, 0.2, and 0.1%). All solutions were sonicated for 30 min and then allowed to stand for 48 h with occasional sonication to ensure maximum solubility of the flavonoid in the solution of interest. After standing for a period of 24 h, the solutions were carefully decanted. The SDS titrant solutions of 80 mM fixed concentration were prepared directly from PSS water solutions and/or PSS + QN water solutions.

Methods

Titration experiments

Microcalorimetric titration measurements have been carried out using an isothermal calorimeter (model number CSC 4200, ±0.01 μW accuracy, from Calorimetry Sciences Corporation) having a 1300-μL titration cell and a 250-μL syringe, with continuous/constant stirring at 35 °C. A concentrated SDS + PSS solution into PSS or concentrated SDS + PSS + QN into PSS + QN solution was titrated in the form of 16 injections of 15 μL each. In all cases, x% PSS + QN solution refers to a solution having x% of PSS with added QN. Similarly, x% PSS + SDS + QN solution refers to a solution having x% of PSS and 80 mM SDS with added QN.

Batch experiments

Microcalorimetric Batch measurements have been carried out using an isothermal calorimeter (model number CSC 4200, ±0.01 μW accuracy, from Calorimetry Sciences Corporation) having a 1300-μL reaction vessel fitted with high speed stirrer and manual operating push button sample holder. For each experiment, a 0.5-mg quantity of solid sample (quercetin) was placed in the sample holder. The reaction vessel, already filled with 1 mL of PSS or a PSS/SDS solution in water, was assembled together with the

sample holder and stirrer. The assembly was then loaded into the microcalorimeter and was allowed to equilibrate overnight at 308.15 K and at stirring rate of 300 rpm. Immediately after equilibration of the instrument, the solid sample was injected into the reaction vessel. The instrument was calibrated repeatedly prior to measurements and the deconvolution was turned off with low gain settings for the batch experiments. A number of the titrations were performed in triplicate; the deviations reported in the measured enthalpy values represent the maximum deviation from the average of the three runs. As these maximum deviations changed little in the presence of the added flavonoid and polymer, the range quoted for the enthalpy values on the graphs represents the maximum deviation observed in our triplicate runs.

The raw data obtained from the instrument for all experiments was processed using BindWork 3.1 software provided by Calorimetry Sciences Corp.

Results and discussion

A typical enthalpogram for the dilution of 0.1% PSS + SDS + QN titrant solution into a 0.1 PSS + QN solution is given in Fig. 2a. Integrated data obtained from this ITC tracing are plotted in Fig. 2b; similar data were obtained for all the other systems. The enthalpograms are typical of the heat of dilution curves for polymer/surfactant systems; there are three distinct regions in the heat flow versus surfactant concentration profile. The initial region corresponds to the dilution of a very concentrated surfactant solution in the micelles form or the polymer/surfactant aggregates into water, resulting in the breakup of the micelles or aggregates into monomers and interactions between the monomers. The steep upward rise starts with the beginning of formation of micelles or polymer/surfactant aggregates upon further addition of concentrated surfactant or surfactant polymer solution. The final region represents the heat flow as the more concentrated micelle or complex containing solution is diluted to a lower aggregate concentration, with the monomer concentration remaining essentially constant. In the critical micellar concentration (cmc) or critical aggregation concentration region (cac), the heat flows are due to the dilution of the aggregate-containing solution to concentrations near the cmc (or cac), resulting in the partial ionization of the aggregates and a decrease in the inter-micellar interactions, or the interactions between the polymer and the surfactant. In this cmc (or cac) region, the transition to the complexes or micelles from the monomers is gradual, meaning that the formation of the aggregates is not a true phase separation.

One of the most widely used models for the theoretical treatment of a surfactant/polyelectrolyte system is the

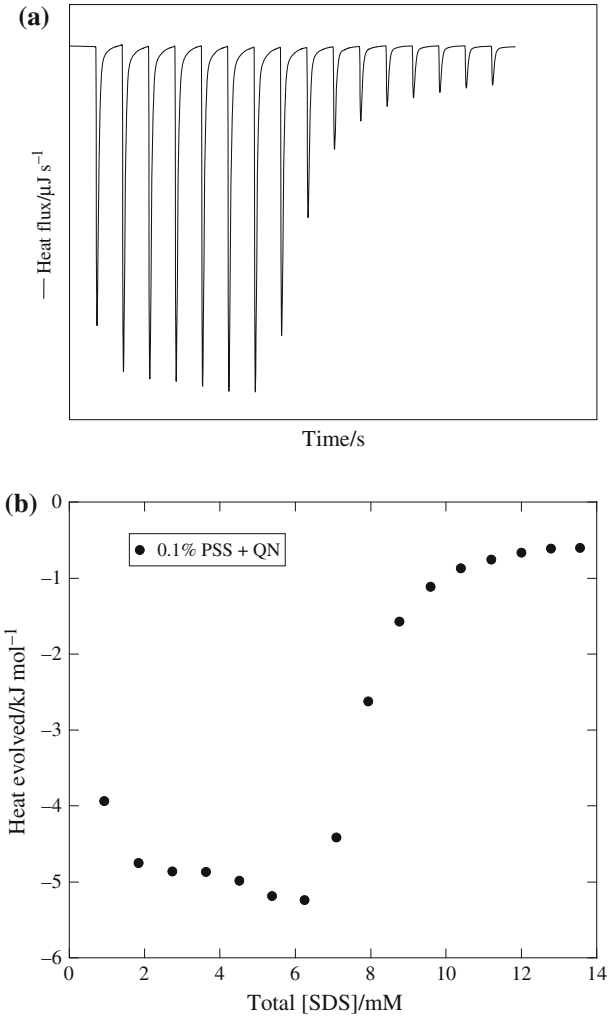

Fig. 2 Sample ITC enthalpograms for dilution of SDS + PSS + QN solution into 0.1% PSS + QN (**a**) raw data recorded on the instrument and (**b**) integrated heat obtained for the raw data

Satake–Yang adsorption model, which is based on the Zimm–Bragg theory for the helix-coil transition in biopolymers. In the Satake–Yang model, the cooperative binding of small ions (e.g., surfactants) with a polyelectrolyte is described as a linear rod containing a specified number of binding sites where the surfactant can adsorb either cooperatively or in a non-cooperative manner. Consider the following binding equilibria

$$\mathrm{OO} + \mathrm{S}^- \overset{K}{\rightleftharpoons} (\mathrm{OS}) \quad (1)$$

$$\mathrm{OS} + \mathrm{S}^- \overset{Ku}{\rightleftharpoons} (\mathrm{SS}) \quad (2)$$

where OO represents a binding site on the polymer, S^- is the anionic surfactant, and S is an occupied site on the polymer. The equilibrium constant, *Ku*, represents the binding of the surfactant to an adjacent site already occupied by a

surfactant (cooperative adsorption); if this site (as described by Eq. 1) is vacant, then the adsorption is non-cooperative and is described by the equilibrium constant K. The parameter u is known as the cooperativity parameter and is determined by the hydrophobic interactions between two adjacently bound surfactant molecules. The average fractional coverage can be expressed in terms of the quantity, the free surfactant concentration, C_S, [38].

$$\beta = \frac{1}{2}\left[1 + \frac{KuC_S - 1}{\sqrt{(1 - KuC_S)^2 + (4KuC_S/u)}}\right] \tag{3}$$

Both Ku and u can be calculated from the following equations

$$Ku = \frac{1}{C_S(\beta = 0.5)} \tag{4}$$

$$u = 16\left(\frac{d\beta}{d\ln\ C_S}\right)^2_{\beta=0.5} \tag{5}$$

An illustrative model sigmoidal isotherm generated from Eq. 3 is shown in Fig. 3. The cac is marked at the upturn in the binding isotherm. Using a binding isotherm equation like the Satake–Yang model, the theoretical ITC curve can be expressed analytically in terms of the binding parameters, Ku, u, and the molar enthalpies of cooperative and non-cooperative binding [4].

$$\Delta\overline{H}_{calc} = C_P \times \frac{\partial\left(\sum_J \Delta\overline{H}_J^{total} \Big/ \Delta\overline{H}_{sat}\right)}{\partial C_S^{free}} \Delta\overline{H}_{avg} \tag{6}$$

Here, C_P is the polyelectrolyte binding site concentration and ΔH_{calc} is the calculated molar enthalpy of adsorption.

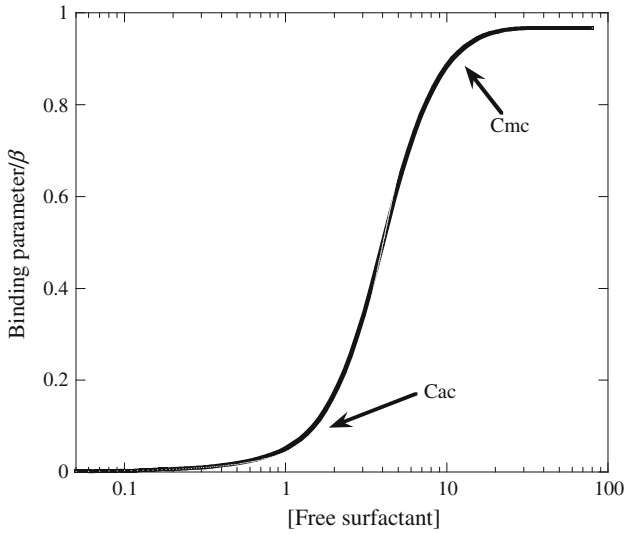

Fig. 3 Satake–Yang polymer/surfactant binding isotherm model curve. The *arrows* indicate the critical aggregation concentration (cac) and critical micellar concentration (cmc)

$\Delta\overline{H}_J^{total}$ and $\Delta\overline{H}_{sat}$ represent the summation of the observed enthalpy changes up to the specified injection concentration and to the saturation point of the polyelectrolyte, respectively. The ΔH_{avg} is a function of the molar enthalpies of cooperative $\left(\Delta\overline{H}_C\right)$ and non-cooperative adsorption $\left(\Delta\overline{H}_N\right)$ and the fraction of cooperatively adsorbed surfactant molecules, f.

$$\Delta\overline{H}_{avg} = \Delta\overline{H}_C \times f + \Delta\overline{H}_N \times (1 - f) \tag{7}$$

The measured value for the heats of dilution as a function of the total surfactant concentration therefore contain significant contributions from the heats of cooperative and non-cooperative binding, respectively. If we assume negligible contributions from the heat of dilution of the polymer, then the observed enthalpy change can be readily used to approximate β by dividing $\Delta\overline{H}_J^{total}$ for each specific injection by $\Delta\overline{H}_{sat}$. Typically, the enthalpy of cooperative binding is calculated from the observed enthalpy values at high concentration of surfactant (i.e., where the polymer chains are assumed to be fully saturated with surfactant molecules); the non-cooperative binding enthalpy is obtained from the experimentally observed binding enthalpies at very low surfactant concentrations, where the probability of a surfactant molecule binding adjacently to another surfactant molecule would be negligible. It is presumed here the Satake–Yang binding isotherm is not overly sensitive to deviations in the enthalpies of cooperative and noncooperative binding [4]. The β value, approximated from the above method, can be used to evaluate the free surfactant concentration as follows:

$$C_S^{total} = C_S^{free} + C_P\beta(C_S) \tag{8}$$

The C_S^{free} values obtained via Eq. 8 are used to evaluate the parameters Ku and u from Eqs. 3–5. Once the molar enthalpies of cooperative and non-cooperative adsorption are estimated from the ITC data, the concentrations of the free and bound surfactant, the theoretical ITC curve is generated using the concentrations of the free and bound surfactant generated from the Satake–Yang binding isotherm and Eq. 8. The difference among the theoretical curves generated in this fashion, and the experimental enthalpies were minimized via least squares fitting. A comparison between experimental and the calculated values of the adsorption isotherms estimated using the calorimetric data with the Satake–Yang model is presented in Fig. 4a–c. It is clearly evident from Fig. 4a–c that the polymer/surfactant systems studied here do not deviate greatly from the Satake–Yang model, although some deviations from the experimental value of the heats of dilution are evident at higher surfactant concentrations, which can be attributed to interpolymer interactions, or the heat effects associated with the formation of free micelles

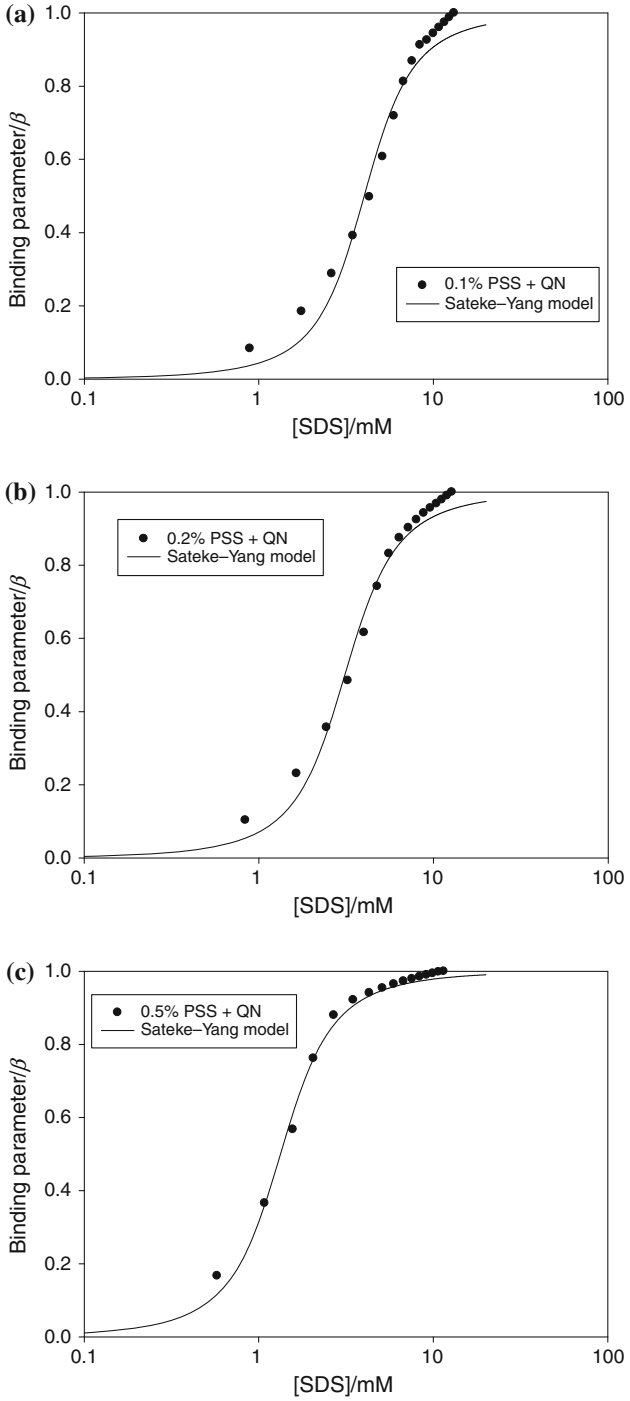

Fig. 4 Polymer/surfactant binding isotherms for **a** 0.1% PSS + QN solution, **b** 0.2% PSS + QN solution, and **c** 0.5% PSS + QN solution. The *solid line* represents the fit to the Satake–Yang model

after the polymer is saturated with surfactant. It is noted that the nearest neighbor model described here is a substantial oversimplification of the formation of these polymer/surfactant aggregates, as it ignores complex phenomena such as conformation changes, the formation of larger aggregates, as well as the possibility of bilayer

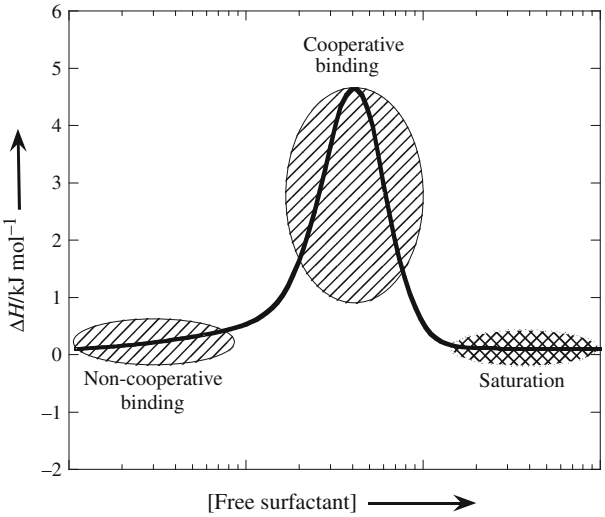

Fig. 5 Schematic representation of an ITC curve obtained from a generic polymer/surfactant binding process

adsorption. However, according to Lapitsky et al. [4], even under these conditions, the calorimetric method can still yield useful information about the adsorption behavior of the surfactant to the polymer.

The ITC signal due to the interaction of the surfactant with the polyelectrolyte can be obtained by subtracting the heat of dilution for the surfactant (SDS in this case) into water from the heat of dilution of SDS + PSS titrant into PSS solution or SDS + PSS + QN titrant into PSS + QN solutions. Under ideal conditions, an enthalpogram obtained in this fashion should look like the one represented in Fig. 5. Such an enthalpogram is divisible into three regions. The first of these is a plateau at low surfactant concentrations, representing the region where there are few surfactant molecules interacting with the polymer. In this region, the binding can be considered to be mostly non-cooperative as there should be very few nearest neighbors when the surfactant interacts with the polymer (Eq. 2). The second region comprises a peak at intermediate surfactant concentrations, and the third region is characterized by a plateau at high concentrations of surfactant, where the enthalpy approaches zero. The peak in the intermediate region is due to the cooperative binding of the surfactant to the polymer (Eq. 1), whereas the binding enthalpy at high surfactant concentration approaches zero when all the available sites on the polyelectrolyte are occupied, and no further surfactant adsorption takes place. The experimental enthalpies have been fitted to a theoretical curve obtained from Eq. 6 via least-squares analysis (Fig. 6a–c) in order to obtain the binding parameters (both Ku and u). The fitted binding parameter can be used to estimate the standard molar Gibbs free energy of cooperative and non-cooperative binding (ΔG_C and ΔG_N, respectively) as follows [39].

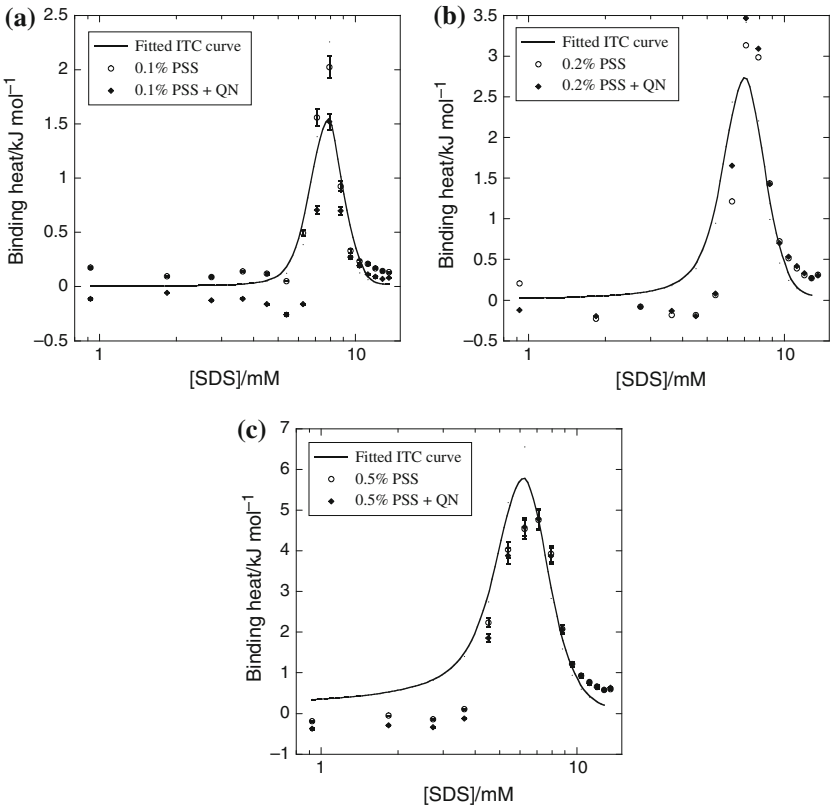

Fig. 6 Various plots of fitted ITC data for **a** 0.1% PSS + QN and 0.1% PSS solutions, **b** 0.2% PSS + QN and 0.2% PSS solutions, and **c** 0.5% PSS + QN and 0.5% PSS solutions

$$\Delta G_C = -RT \ln(Ku) \quad (9)$$

$$\Delta G_N = -RT \ln(Ku/u) \quad (10)$$

As was stated above, in estimating ΔG_N, it is assumed that in the limit of very low surfactant concentration, the adsorption is exclusively non-cooperative and the fractional coverage is negligible.

The values of ΔG_C and ΔG_N obtained for the PSS/SDS/QN and PSS/SDS systems are listed in Table 1. One can see that the values of ΔG_C and ΔG_N are more negative for PSS/QN/SDS than the PSS/SDS systems. Both ΔG_C and ΔG_N are almost equally affected by the presence of QN. At this point, it can be concluded that the presence of QN is increasing the polymer/surfactant binding through hydrophobic interactions, and the effect is very similar to that of an insoluble dye [1, 39]. Furthermore, the values of ΔG_N are more negative than ΔG_C. When the PSS/SDS/QN systems are compared to the PSS/SDS systems, it indicates that the non-cooperative binding is more favorable than cooperative binding, which is likely due to the differences in the electrostatic effects of binding as more surfactant molecules interact with the polymer. It is also evident in Fig. 6 that the experimental data is deviating from the fitted line in the non-cooperative binding area and these deviations are almost equal for systems with and without QN, except for the 0.1% PSS concentration systems where experimental points are deviating far more in the case of the 0.1% PSS/SDS/QN system compared to the 0.1% PSS/SDS systems. These deviations can be explained by taking into account the various interactions that occur during polymer/surfactant binding. The polymer/surfactant binding is governed by several contributing factors, such as charge effects, chain flexibility, the pH of the solution, and the chemical nature of charged sites [40, 41]. For oppositely charged

Table 1 The values of the binding parameter/Ku, adsorption cooperativity/u, and Gibbs free energy of cooperative/ΔG_C, and non-cooperative/ΔG_N adsorption, evaluated from ITC measurements taken at 308.15 K for all systems

% PSS/w/v%	Ku/mM^{-1}	u	ΔG_C^a/kJ mol^{-1}	ΔG_N/kJ mol^{-1}
PSS/QN/SDS				
0.1%	0.249	8.787	−26.81	−31.54
0.2%	0.322	7.839	−26.25	−30.73
0.5%	0.750	7.734	−24.40	−28.86
PSS/SDS				
0.1%	0.461	7.803	−25.46	−29.94
0.2%	0.311	8.289	−26.32	−30.92
0.5%	0.762	7.555	−24.37	−28.77

[a] Note error in Gibbs energies = ±0.05 kJ mol^{-1}

polymers and surfactants, the binding is controlled mainly through electrostatic interactions [42–44], while for non-ionic-surfactant/ionic-polymer and similarly charged polymer/surfactant systems, the binding is mainly governed by hydrogen bonding and hydrophobic interactions. Additionally, it has been shown that a change in pH affects the polymer/surfactant binding for all combinations of polymer and surfactant [45, 46]. Sometimes the pH change is brought about by the added surfactant and this can lead to a change in the manner in which the polymer/surfactant forms the complex [47, 48]. Four sets of interactions are expected for PSS/SDS/QN systems vis-à-vis interaction between PSS–QN, SDS–QN, SDS–PSS, and PSS–PSS. The PSS–PSS interactions become apparent only at a very high polymer concentration. The binding isotherms in this case have been constructed on the basis of SDS–PSS interactions. At low PSS concentration, QN competes with the adsorption of the SDS molecules, mainly due to hydrophobic interactions between the polymer and the flavonoid. Under these circumstances, the binding between PSS and SDS is not purely non-cooperative; this leads to a deviation of the experimental enthalpy data from the theoretical curve generated via application of the Satake–Yang model (Fig. 6a). For the systems having high concentrations of PSS, deviations from the theoretical curve are almost equal for the systems with and without QN (Fig. 6b, c). This is mainly due to the fact that inter-polymer associations give rise to additional cooperativity from favorable hydrophobic inter-polymer interactions which can override the effect of any added QN.

The free energy change for any physical process has contributions from both the enthalpy change and the entropy change of the process; therefore, it becomes important to understand the energetics of the polymer/surfactant binding process. One way to study the energetics of PSS/SDS binding is to carry out batch microcalorimetry experiments. The batch microcalorimetric experimental technique is a tested method for the determination of enthalpies of dissolution, $\Delta_{sol}H$, of small amounts of easily or slightly soluble solids. In this case, we examined the differences in the heats of dissolution of solid QN into the polymer/surfactant solution in the presence of increasing surfactant concentration at three concentrations of PSS. For these experiments, the batch delivery system, an add-on option for the Calorimetry Sciences Corporation model 4200 ITC, was used. The heats of dissolution ($\Delta_{sol}H$) of QN into various PSS/water systems with an SDS concentration above the cmc (i.e., the cooperative binding region), an SDS concentration below the cmc (the non-cooperative binding region), and with no SDS in the solution were measured. The heats of dissolution for all systems have been given in Table 2; Fig. 7 shows the variation of heat of dissolution of QN into various PSS/water systems against the concentration of SDS. One can see that the values for heat of dissolution are exothermic for all systems, which means the dissolution of QN into pure PSS and PSS/SDS is an enthalpically favored process. Furthermore, the heats of dissolution are found to be more negative for the low SDS concentration systems in all three cases, indicating that the QN interactions are more favored in the non-cooperative binding region. Internal comparisons among all the concentrations of PSS in water indicate that the heat of dissolution is more negative for the system with the minimum amount of PSS, i.e., the 0.1% PSS/water system. These observations favor the values of the free energy of non-cooperative binding obtained from the Satake–Yang model (Table 1). As well, surfactant addition has a minimum

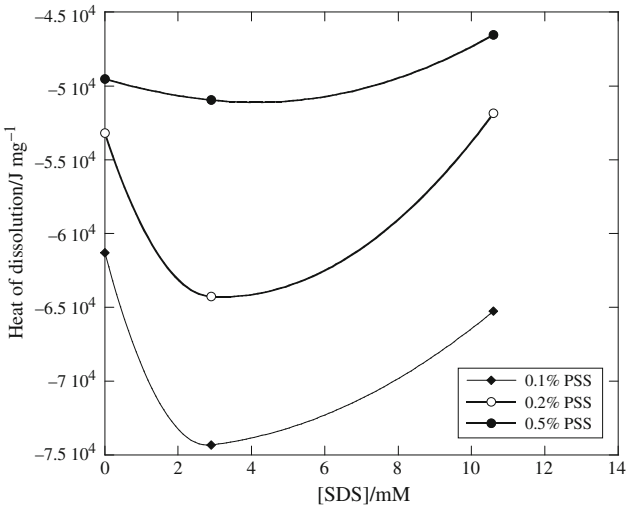

Fig. 7 Variation of the heat of dissolution ($\Delta_{sol}H$) of solid quercetin versus the total SDS concentration for various amounts of PSS in water

Table 2 The values for the heat of dissolution, $\Delta_{sol}H$/J mg^{-1} of QN, in various solutions having different concentrations of PSS and SDS at 308.15 K and 300 rpm

SDS concentration/mM	$\Delta_{sol}H$ for 0.1% PSS/J mg^{-1}	$\Delta_{sol}H$ for 0.2% PSS/J mg^{-1}	$\Delta_{sol}H$ for 0.5% PSS/J mg^{-1}
0.000	−61300	−53194	−49528
2.900	−74318	−64270	−50960
10.600	−65252	−51856	−46538

effect on the 0.5% PSS/water system. All these observations collectively indicate that the presence of QN favors the PSS/SDS interactions. Also, these interactions are more enthalpically favored for the systems where the hydrophobic nature of QN is retained. The latter conclusion is also drawn from the fact that PSS in water provides an alkaline medium that in turn causes the deprotonation of QN. Hence, at higher PSS concentrations, QN interacts with PSS/SDS through ionic interactions instead of purely hydrophobic interactions.

Conclusions

Isothermal titration calorimetry and batch calorimetry have been used to study the effect of the addition of an antioxidant, quercetin, on polymer/surfactant interactions. A modified Satake–Yang model has been used to evaluate the various binding parameters including the Gibbs free energy of cooperative and non-cooperative binding. It has been observed that the presence of QN leads to an increase in polymer/surfactant binding. Furthermore, both cooperative and non-cooperative binding are equally affected and this effect is visible only under conditions of low polymer concentration.

Acknowledgements The authors thank NSERC (Discovery Grant, D.G.M; Research Capacity Development Grant, StFX), the Atlantic Innovation Fund, and the St FX University Council for Research for the financial support of this research.

References

1. Hayakawa K, Shinohara S, Sasawaki S, Satake I, Kwak JCT. Solubilization of water-insoluble dyes by polyion/surfactant complexes. Bull Chem Soc Jpn. 1995;68:2179–85.
2. Wang C, Tam KC. Interactions between poly(acrylic acid) and sodium dodecyl sulfate: isothermal titration calorimetric and surfactant ion-selective electrode studies. J Phys Chem B. 2005;109:5156–61.
3. Haldar B, Chakrabarty A, Mallick A, Mandal MC, Das P, Chattopadhyay N. Fluorometric and isothermal titration calorimetric studies on binding interaction of a telechelic polymer with sodium alkyl sulfates of varying chain length. Langmuir. 2006;22:3514–20.
4. Lapitsky Y, Parikh M, Kaler EW. Calorimetric determination of surfactant/polyelectrolyte binding isotherms. J Phys Chem B. 2007;111:8379–87.
5. Cliff MJ, Gutierrez A, Ladbury JE. A survey of the year 2003 literature on applications of isothermal titration calorimetry. J Mol Recognit. 2004;17:513–23.
6. Velázquez Campoy A, Freire E. ITC in the post-genomic era…? Priceless. Biophys Chem. 2005;115:115–24.
7. Saboury A. Binding isotherm determination by isothermal titration calorimetry. J Therm Anal Calorim. 2004;77:997–1004.
8. Scott MJ, Jones MN. The interaction of phospholipid liposomes with zinc citrate particles: a microcalorimetric investigation. Colloids Surf A. 2001;182:247–56.
9. Hertog MGL, Hollman PCH, van de Putte B. Content of potentially anticarcinogenic flavonoids of tea infusions, wines, and fruit juices. J Agric Food Chem. 1993;41:1242–6.
10. Hertog MGL, Hollman PCH, Katan MB. Content of potentially anticarcinogenic flavonoids of 28 vegetables and 9 fruits commonly consumed in the Netherlands. J Agric Food Chem. 1992;40:2379–83.
11. Takahama U. Suppression of lipid photoperoxidation by quercetin and its glycosides in spinach chloroplasts. Photochem Photobiol. 1983;38:363–7.
12. Cheng F, Breen K. On the ability of four flavonoids, baicilein, luteolin, naringenin, and quercetin, to suppress the fenton reaction of the iron-ATP complex. Biometals. 2000;13:77–88.
13. Bors W, Saran M. Radical Scavenging by flavonoid antioxidants. Free Radical Res. 1987;2:289–94.
14. Cook NC, Samman S. Flavonoids—chemistry, metabolism, cardioprotective effects, and dietary sources. J Nutr Biochem. 1996;7:66–76.
15. Middleton E Jr, Kandaswami C, Theoharides TC. The effects of plant flavonoids on mammalian cells: implications for inflammation, heart disease, and cancer. Pharmacol Rev. 2000;52:673–751.
16. Solimani R. The flavonols quercetin, rutin and morin in DNA solution: UV–vis dichroic (and mid-infrared) analysis explain the possible association between the biopolymer and a nucleophilic vegetable-dye. Biochim Biophys Acta. 1997;1336:281–94.
17. Kitson TM, Kitson KE, Moore SA. Interaction of sheep liver cytosolic aldehyde dehydrogenase with quercetin, resveratrol and diethylstilbestrol. Chem Biol Interact. 2001;130–132:57–69.
18. Dangles O, Dufour C, Manach C, Morand C, Remesy C. Binding of flavonoids to plasma proteins. Methods Enzymol. 2001;335:319–33.
19. Frazier RA, Papadopoulou A, Mueller-Harvey I, Kissoon D, Green RJ. Probing protein-tannin interactions by isothermal titration microcalorimetry. J Agric Food Chem. 2003;51:5189–95.
20. Deaville ER, Green RJ, Mueller-Harvey I, Willoughby I, Frazier RA. Hydrolyzable tannin structures influence relative globular and random coil protein binding strengths. J Agric Food Chem. 2007;55:4554–61.
21. Diab C, Winnik FM, Tribet C. Enthalpy of interaction and binding isotherms of non-ionic surfactants onto micellar amphiphilic polymers (amphipols). Langmuir. 2007;23:3025–35.
22. Kujawa P, Raju BB, Winnik FM. Interactions in water of alkyl and perfluoroalkyl surfactants with fluorocarbon- and hydrocarbon-modified poly(N-isopropylacrylamides). Langmuir. 2005;21:10046–53.
23. Su J, Liu S, Joshi S, Lam Y. Effect of SDS on the gelation of hydroxypropylmethylcellulose hydrogels. J Therm Anal Calorim. 2008;93:495–501.
24. Bai G, Castro V, Nichifor M, Bastos M. Calorimetric study of the interactions between surfactants and dextran modified with deoxycholic acid. J Therm Anal Calorim. 2010;100:413–22.
25. Li Y, Fei G, Honglin Z, Zhen L, Liqiang Z, Ganzuo L. Effects of long-chain alcohols on the micellar properties of anionic surfactants in non-aqueous solutions by titration microcalorimetry. J Therm Anal Calorim. 2009;96:859–64.
26. Coldren BA, Warriner H, van Zanten R, Zasadzinski JA. Lamellar gels and spontaneous vesicles in catanionic surfactant mixtures. Langmuir. 2006;22:2465–73.
27. Taheri-Kafrani A, Bordbar A. Energitics of micellizaion of sodium n-dodecyl sulfate at physiological conditions using isothermal titration calorimetry. J Therm Anal Calorim. 2009;98:567–75.
28. Zidelkheir B, Abdelgoad M. Effect of surfactant agent upon the structure of montmorillonite. J Therm Anal Calorim. 2008;94:181–7.

29. Lee VA, Craig RG, Filisko FE, Zand R. Microcalorimetry of the adsorption of lysozyme onto polymeric substrates. J Colloid Interface Sci. 2005;288:6–13.
30. Zajac J. Adsorption microcalorimetry used to study interfacial aggregation of quaternary ammonium surfactants (zwitterionic and cationic) on powdered silica supports in dilute aqueous solutions. Colloids Surf. 2000;167:3–19.
31. Singh S, Caram-Lelham N. Thermodynamis of k-carrageenan-amphiphilic drug interaction as influenced by specific counterions and temperature: a microcalorimetric and viscometric study. J Colloid Interface Sci. 1998;203:430–46.
32. Lu L, Cai J, Frost R. Desorption of stearic acid upon surfactant adsorbed montmorillonite. J Therm Anal Calorim. 2010;100: 141–4.
33. De Lisi R, Lazzara G. Aggregation in aqueous media of tri-block copolymers tuned by the molecular selectivity of cyclodextrins. J Therm Anal Calorim. 2009;97:797–803.
34. Rezaei Behbehani G, Mirzaie M. A high performance method for thermodynamic study on the binding of copper ion and glycine with Alzheimer's amyloid β peptide. J Therm Anal Calorim. 2009;96:631–5.
35. Lira A, Nanclares D, Neto A, Marchetti J. Drug–polymer interaction in the all-trans retinoic acid release from chitosan microparticles. J Therm Anal Calorim. 2007;87:899–903.
36. Liu W, Guo R. Interaction between flavonoid, quercetin and surfactant aggregates with different charges. J Colloid Interface Sci. 2006;302:625–32.
37. Bordbar A, Hosseinzadeh R, Norozi I M. Interaction of a homologous series of n-alkyl trimethyl ammonium bromides with eggwhite lysozyme. J Therm Anal Calorim. 2007;87:453–6.
38. Satake I, Yang JT. Interaction of sodium decyl sulfate with poly(L-ornithine) and poly(L-lysine) in aqueous solution. Biopolymers. 1976;15:2263–75.
39. Santerre JP, Hayakawa K, Kwak JCT. A study of the temperature dependence of the binding of a cationic surfactant to an anionic polyelectrolyte. Colloids Surf. 1985;13:35–45.
40. Hayakawa K, Kwak JCT. Surfactant–polyelectrolyte interactions. 1. Binding of dodecyltrimethylammonium ions by sodium dextran sulfate and sodium poly(styrenesulfonate) in aqueous solution in the presence of sodium chloride. J Phys Chem. 1982;86:3866–70.
41. Hayakawa K, Santerre JP, Kwak JCT. Study of surfactant–polyelectrolyte interactions. Binding of dodecyl- and tetradecyltrimethylammonium bromide by some carboxylic polyelectrolytes. Macromolecules. 1983;16:1642–5.
42. Wang C, Tam KC. Interaction between polyelectrolyte and oppositely charged surfactant: effect of charge density. J Phys Chem B. 2004;108:8976–82.
43. Wang C, Tam KC, Jenkins RD, Tan CB. Interactions between methacrylic acid/ethyl acrylate copolymers and dodecyltrimethylammonium bromide. J Phys Chem B. 2003;107:4667–75.
44. Burrows HD, Tapia MJ, Silva CL, Pais AACC, Fonseca SM, Pina J, de Melo JS, Wang Y, Marques EF, Knaapila M, Monkman AP, Garamus VM, Pradhan S, Scherf U. Interplay of electrostatic and hydrophobic effects with binding of cationic Gemini surfactants and a conjugated polyanion: experimental and molecular modeling studies. J Phys Chem B. 2007;111:4401–10.
45. Chandar P, Somasundaran P, Turro NJ. Fluorescence probe investigation of anionic polymer-cationic surfactant interactions. Macromolecules. 1988;21:950–3.
46. Yoshida K, Dubin PL. Complex formation between polyacrylic acid and cationic/nonionic mixed micelles: effect of pH on electrostatic interaction and hydrogen bonding. Colloids Surf A. 1999;147:161–7.
47. Kiefer JJ, Somasundaran P, Ananthapadmanabhan KP. Interaction of tetradecyltrimethylammonium bromide with poly(acrylic acid) and poly(methacrylic acid). Effect of charge density. Langmuir. 1993;9:1187–92.
48. Shimizu T. Changes of pH and counterion activity during the binding process of cationic surfactants to carboxylic polyions. Colloids Surf A. 1994;84:239–48.